The Hantavirus Nucleocapsid Protein Recognizes Specific Features of the Viral RNA Panhandle and Is Altered in Conformation upon RNA Binding

M. A. Mir and A. T. Panganiban*

Department of Molecular Genetics and Microbiology, University of New Mexico Health Sciences Center, Albuquerque, New Mexico

Hantaviruses are tripartite negative-sense RNA viruses and members of the *Bunyaviridae* family. The nucleocapsid (N) protein is the principal structural component of the viral capsid. N forms a stable trimer that specifically recognizes the panhandle structure formed by the viral RNA termini. We used trimeric glutathione *S*-transferase (GST)-N protein and small RNA panhandles to examine the requirements for specific recognition by Sin Nombre hantavirus N. Trimeric GST-N recognizes the panhandles of the three viral RNAs (S, M, and L) with high affinity, whereas the corresponding plus-strand panhandles of the complementary RNA are recognized with lower affinity. Based on analysis of nucleotide substitutions that alter either the higher-order structure of the panhandle or the primary sequence of the panhandle, both secondary structure and primary sequence are necessary for stable interaction with N. A panhandle 23 nucleotides long is necessary and sufficient for high-affinity binding by N, and stoichiometry calculations indicate that a single N trimer interacts with a single panhandle. Surprisingly, displacement of the panhandle structure away from the terminus does not eliminate recognition by N. The binding of N to the panhandle is an entropy-driven process resulting in initial stable N-RNA interaction followed by a conformational change in N. Taken together, these data provide insight into the molecular events that take place during interaction of N with the panhandle and suggest that specific high-affinity interaction between an RNA binding domain of trimeric N and the panhandle is required for encapsidation of the three viral RNAs.

The members of the *Hantavirus* genus of the family *Bunyaviridae* are spherical, enveloped viruses containing tripartite negative-sense RNA as their genome (37). The three genomic RNA segments, designated L, M, and S, encode an RNA-dependent RNA polymerase, envelope glycoproteins (G1 and G2), and nucleocapsid (N) protein, respectively. Hantavirus infections can cause two serious and often fatal human diseases, hemorrhagic fever with renal syndrome and hantaviral pulmonary syndrome, characterized by lung damage and cardiac dysfunction (36). Humans are infected with hantaviruses from rodent reservoirs that are persistently infected without signs of disease (38).

The initial steps in hantavirus infection require binding of the G1 and/or G2 protein to β3 integrin (9) or other cell surface receptors, followed by virus entry and uncoating. After entry, L-protein mediates transcription of minus-strand RNA, resulting in plus-stranded mRNA in the cytoplasm, apparently with an orthomyxovirus-like cap-snatching mechanism (7, 8, 16). Following viral mRNA translation, transcription shifts from mRNA to plus-strand complementary RNA and de novo minus-strand viral RNA synthesis concomitant with the formation of ribonucleoprotein structures (7, 16, 37). The ribonucleoproteins appear to be composed of viral RNA, N protein, and presumably viral polymerase and accumulate on the cytoplasmic side of intracellular membranes, possibly through interaction with the G1 ands G2 proteins (10, 28). Additional evidence suggests that hantavirus assembly can occur at the plasma membranes of infected cells (10, 32). It has also been shown that transport of newly synthesized ribonucleoproteins to the plasma membrane, where Black Creek canal hantavirus is assembled, could be mediated through actin filaments (33).

The viral N protein is central to the hantaviral replication cycle. The activity and biological function of N protein in the viral life cycle are proposed to depend on differential interaction with minus-strand viral RNA, plus-strand complementary RNA, and the mRNA. Cell culture-based experiments with bunyamwera virus indicate that the formation of intracellular RNA-nucleocapsid complexes is specific for full-length viral RNA or complementary RNA molecules, since no mRNA molecules are observed in nucleocapsids (18), indicative of a role for N during both complementary RNA and viral RNA synthesis. The encapsidation process must necessarily result in the preferential packaging of viral RNA into nucleocapsids destined for particle exit.

Electron microscopic analysis indicates that the termini of the phlebovirus Uukuniemi virus interact to form circular structures that dissociate under denaturing conditions (14). Furthermore, such circular RNA structures for other members of the *Bunyaviridae* have also been observed in the presence of nucleoprotein complexes, further suggesting that intramolecular association of the viral RNA termini forms in vivo (25, 29, 31). All members of the *Bunyaviridae* family contain terminal nucleotide sequences that could facilitate the association of termini through the formation of short panhandles. Moreover, the termini of both viral RNA and complementary RNA may

* Corresponding author. Mailing address: Department of Molecular Genetics and Microbiology, University of New Mexico Health Sciences Center, Albuquerque, NM 87131. Phone: (505) 272-4214. Fax: (505) 272-9912. E-mail: apanganiban@salud.unm.edu.

undergo substantial antiparallel base-pairing, so both the negative- and positive-sense RNAs could potentially form panhandles of similar stability.

Biochemical and genetic methods indicate that N protein forms trimers that are ostensibly subunits that form the capsid. Based on analysis of peptides derived from Sin Nombre hantavirus, the C-terminal half plus the N-terminal 40 amino acid residues of N protein are responsible for intermolecular N-protein association (1). Similarly, analysis of protein-protein interaction with truncated N mutants in conjunction with a mammalian two-hybrid assay indicates that N-terminal amino acids 1 to 43 are involved in and C-terminal amino acids 393 to 398 (VNHFHL) are essential for homotypic interactions in N protein homodimers and homotrimers in Tula hantavirus (20).

In vitro binding studies have been used to examine the specificity of the interaction between N and its RNA with bacterially expressed, hexahistidine-tagged N from various species from the hantavirus genus (12, 39, 40), the bunyavirus genus (26), and the tospovirus genus (35). Based on this work, hantavirus and bunyavirus N proteins appear to preferentially interact with a target site near the 5′ end of the viral RNA. Recently, it was observed that trimeric glutathione *S*-transferase (GST)-tagged N preferentially binds to the panhandle, an RNA substrate composed of both the 5′ and 3′ ends (23). This specificity for the panhandle appears to be a characteristic of the trimer, as a heterogenous population of N composed of a population of N molecules of mixed subunit composition does not discriminate between the 5′ end and the panhandle. The region of hantavirus N required for RNA binding appears to be situated in the central conserved region from amino acids 175 to 217 (43). However, for the tospovirus genus, the data are consistent with the presence of multiple RNA binding domains (35).

Here we examined the characteristics of the panhandle RNA required for recognition by hantavirus N protein. Recognition of the panhandle by purified trimeric N requires specific features of the panhandle, as reflected by both a requirement for secondary structure and conserved nucleotide sequence. Moreover, binding of the trimeric N protein to the panhandle is an entropy-driven process resulting in the recruitment of one trimer per panhandle and results in a conformational change in the protein. This specific recognition is likely to be a key step in the hantaviral RNA encapsidation process and general to members of the *Bunyaviridae* family.

MATERIALS AND METHODS

Oligonucleotides and enzymes. PCR primers were from Sigma Genosys. All restriction enzymes were from New England Biolabs. Hot Mastertaq polymerase was from Eppendorf. DNase I and T7 transcription reagents were from Invitrogen. All other chemicals were purchased from Sigma. RNA purification kits were from Qiagen.

Expression and purification of trimeric hantavirus GST-N protein. *Sin Nombre* virus nucleocapsid protein derived from strain 77734 (2) was expressed as an N-terminal GST fusion protein in *Escherichia coli*. This protein was denatured and renatured, and stable trimeric GST-N was purified on 10 to 60% sucrose gradients as described in detail previously (23). Freshly prepared trimeric GST-N protein was used for all experiments.

Preparation of RNA substrates. Wild-type S segment panhandle RNA containing 32 nucleotides from both the 5′ and 3′ ends of Sin Nombre virus S segment viral RNA separated by a loop of six uracil residues was synthesized by in vitro transcription with T7 polymerase. We used a single-stranded template sequence (5′-TAGTAGTAGACTCCTTGAGAAGCTACTCGACAAAAAT

TCTTGTTGCTTTTCAAGGAGCATACTACTACTATAGTGAGTCGTATT AGCTAG-3′) containing a T7 promoter juxtaposed to the sequence coding for S segment RNA from Sin Nombre virus strain R11 (4). This single-stranded sequence was amplified by PCR with the primers 5′-CTAGCTAATACGACT-CACTATAGTAGTAG-3′ and 5′-TAGTAGTAGACTCCTTGAGAAGCT-3′. The PCR product was gel purified before use in the T7 transcription reaction.

For the synthesis of the various mutants, we employed the same strategy, incorporating priming oligonucleotides with the appropriate nucleotide changes. The necessary primers or template containing the desired mutations was amplified with PCR, and the amplified DNA was gel purified and used directly in T7 transcription reactions. [^{32}P]CTP-radiolabeled transcripts were produced from different templates according to the manufacturer's protocol with T7 transcription reagents (MBI Fermentase). After transcription, the reaction mixture was digested with DNase I to remove the DNA template. Purification of RNA was performed with Trizol reagent (Qiagen). Purified RNA was stored at −20°C in 20-μl aliquots for up to 2 weeks.

Filter binding assays. Binding reactions were carried out as described previously (23) in binding buffer at a constant concentration of RNA with increasing concentration of purified trimeric GST-N. The reaction mixture was incubated at room temperature for 45 min and filtered through nitrocellulose filters under vacuum. The filters were washed with 10 ml of binding buffer and dried, and the retained RNA was measured with a scintillation counter. Nonspecific retention of RNA was monitored by filtering the complete reaction mixture in the absence of protein. Dissociation constants were calculated by fitting the experimental data points in to a hyperbolic equation with Origin 6 (Microcal). The apparent dissociation constant (K_d) corresponds to the concentration of N protein required to obtain half saturation, assuming that complex formation obeys a simple bimolecular equilibrium.
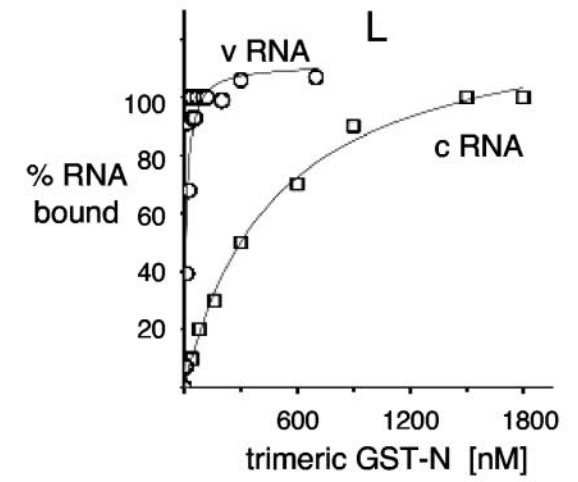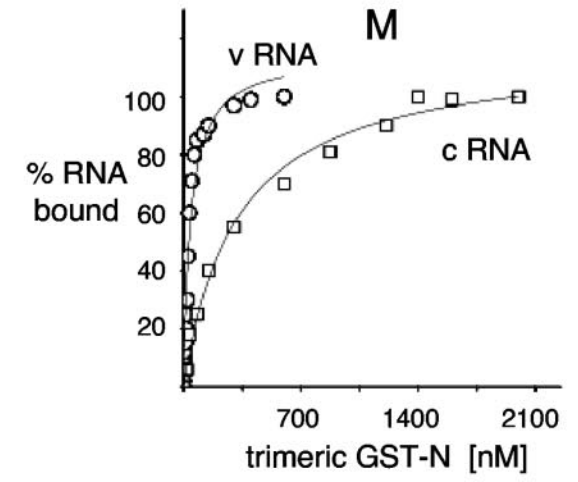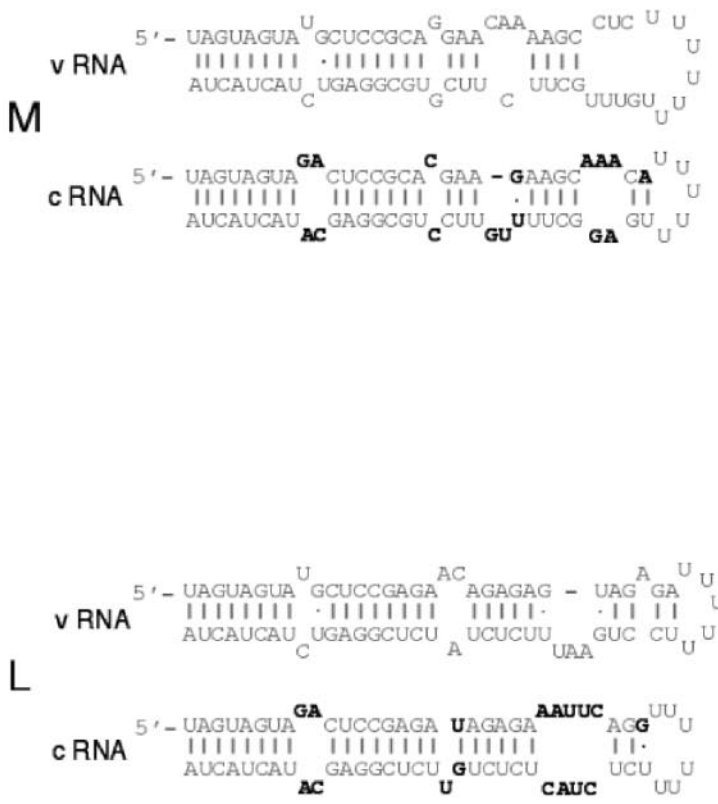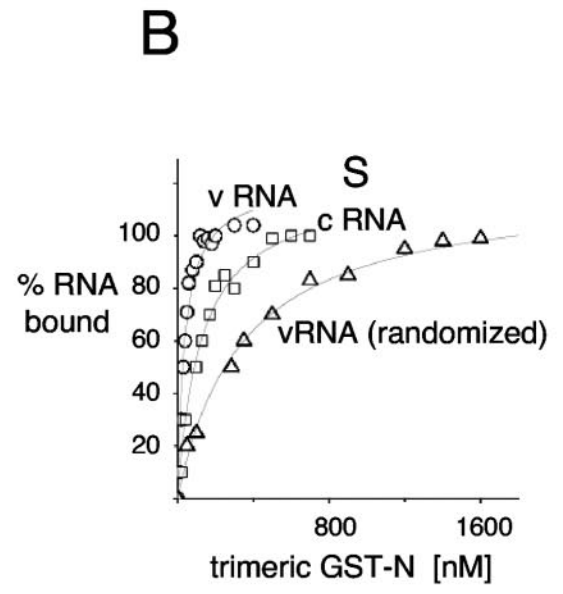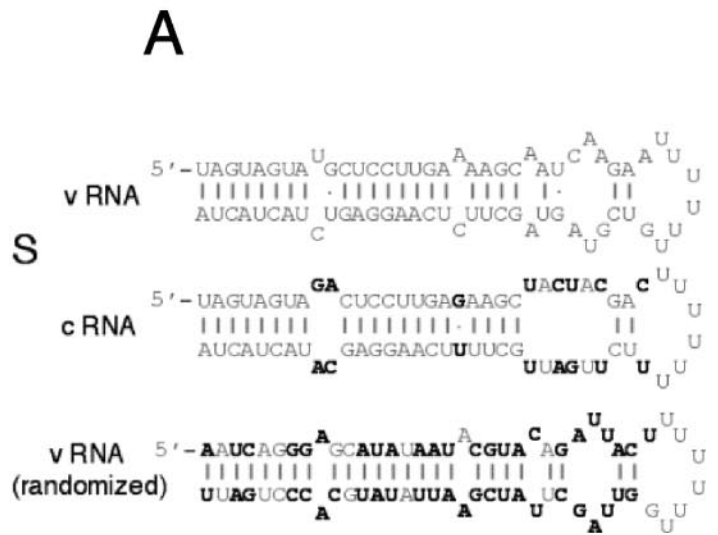
Competition experiments were performed with filter binding assays. A constant concentration of hantavirus GST-N protein (100 nM) was incubated with a constant concentration of [^{32}P]CTP-labeled wild-type panhandle RNA (0.01 nM) and increasing concentrations of competitor RNA. The reaction mixture was incubated at room temperature for 45 min and then filtered through nitrocellulose filters under vacuum as described for the filter binding assay above. The bound wild-type panhandle RNA was plotted against the competitor RNA concentration. Data points were fit by nonlinear curve fit analysis with the Origin 6 program (Microcal).

RNA secondary structure analysis. We examined multiple suboptimal secondary structure plots to identify alternative structures that might be nearly as stable as those shown in Fig. 1 and 2. In addition, we determined the P-num values for each of the nucleotides in the RNAs. The P-num value of a nucleotide is a representation of the number of potentially stable pairing partners for that nucleotide elsewhere in the same RNA. In particular, P-num is a predictive measure of pairing fidelity at suboptimal free energy values (ΔG), and bases with low values can be used parametrically to identify motifs with the highest probability of assuming similar configurations among a series of energetically related structures (17). Thus, when viewed from the context of suboptimal folds, the structures composed of low P-num nucleotides still form and are still composed of bases with the fewest alternative pairing partners (low P-num) (27).

Examination of suboptimal folds indicated that, with the exception of RNA 14, the terminal secondary structures shown in Fig. 1 and 2 are much more thermodynamically stable than alternative suboptimal structures; typically the structures have a ΔG of approximately −30 kcal/mol, whereas the next most likely structure has a negative free energy that is more than 70% of this low minimum free energy. Moreover, the P-num values for most of the nucleotides that constitute the panhandle is either 1 or 0, where paired nucleotides have a value of 1 whereas unpaired nucleotides have a value of 0. Thus, it is highly unlikely that RNAs of alternative secondary structure to that shown constitute a significant proportion of the RNA population.

Calculation of binding stoichiometry. The binding stoichiometry (expressed in terms of number of N molecules bound per RNA panhandle) was estimated from the intersection of two straight lines of a least square fit plot of the increase in bound RNA against the ratio of input concentrations of GST-N protein and RNA (24).

Fluorescence spectroscopic analysis. Structural alterations in the GST-N protein trimer due to its binding with different RNA molecules were monitored by quenching the tryptophan fluorescence of the N protein trimer with acrylamide in the presence and absence of RNA according to the Stern-Volmer equation (22) $F_0/F = 1 + Ksv[Q]$, where F_0 and F are the fluorescence intensities in the absence and presence of quencher, respectively, $[Q]$ is the concentration of quencher, and Ksv is the Stern-Volmer quenching constant. Fluorescence quenching measurements of tryptophan in N protein with acrylamide quencher were made by serial addition of small aliquots of concentrated acrylamide solu-

tion to 1 ml of sample in a cuvette. If the plot of F_0/F versus $[Q]$ is linear, which indicates a single class of fluorophores equally accessible to acrylamide, the value of Ksv can be calculated from the slope of straight line fit to the data points.

Analysis of thermodynamic parameters. Thermodynamic parameters ΔH (van't Hoff enthalpy), ΔS (entropy), and ΔG (free energy) for the association of GST-N protein trimer with wild-type panhandle RNA were calculated with the equations $\ln K_{app} = -\Delta H/RT + \Delta S/R$ and $\Delta G = \Delta H - T\Delta S$, where R and T are the universal gas constant and absolute temperature, respectively, and K_{app} (apparent equilibrium constant $= 1/K_d$) was calculated at three different temperatures (25, 30, and 37°C) by fluorometric titration of GST-N protein trimer with S segment panhandle RNA. The fluorescence spectra of GST-N protein trimer in binding buffer excited at 295 nm were recorded with a Hitachi spectrofluorometer at an excitation and emission band pass of 5 and 10 nm, respectively. Contribution from the binding buffer was subtracted whenever required. The apparent dissociation constant (K_d) corresponds to the concentration of N protein required to obtain half saturation, assuming that complex formation obeys a simple bimolecular equilibrium. ΔH and ΔS were calculated from the slope and intercept of a plot of $\ln K_{app}$ against $1/T$. ΔG was calculated from the third equation after incorporation of the values for ΔH and ΔS obtained from the second equation.

RESULTS

Differential recognition of viral RNA and complementary RNA panhandles by trimeric N. Previously we observed that purified trimeric N recognizes the viral S segment panhandle with specificity (23). We wanted to examine the requirements for recognition of the panhandle by purified trimeric GST-N. The S, M, and L segment hantavirus RNAs can potentially form terminal panhandles of similar secondary structure and slightly variable primary sequence. Moreover, full-length positive-strand complementary RNA would be able to form panhandle structures similar but not identical to those found in the viral RNA (Fig. 1). We purified trimeric GST-N with sucrose gradients and used this freshly purified trimeric protein to examine the affinity of N for RNAs corresponding to the three viral genome panhandle RNAs and their plus-strand complementary RNA panhandle counterparts. In addition, we generated an RNA identical in secondary structure and nucleotide composition but different in sequence from that of S segment viral RNA (viral RNA randomized) (Fig. 1).

Previously we observed that a relatively small RNA composed of the S segment RNA panhandle is sufficient for high-affinity binding by trimeric GST-N protein (23). Thus, we examined the association of trimeric GST-N with small panhandle RNAs containing the terminal 33 nucleotides from both the 5′ and 3′ ends and separated by a 6-nucleotide-long spacer composed of U residues. Depending on sequence length and complexity, RNAs can potentially form multiple

secondary structures. However, on the basis of both analysis of suboptimal RNA folds and P-num analysis (see above) RNAs of secondary structure significantly different from those shown in Fig. 1 are predicted to be highly unlikely.

The results of RNA filter binding experiments with these viral and complementary RNA substrates are shown in Fig. 1, and a summary of the binding data with these panhandle RNAs is shown in Table 1. Each of the viral RNAs corresponding to the three genome segments was recognized with similar high affinity by trimeric GST-N protein. Furthermore, this protein-RNA interaction was stable to increasing NaCl concentrations, indicative of specificity. Interestingly, the binding affinity of the plus-strand complementary RNA panhandles was markedly reduced relative to that of the viral RNAs and sensitive to increased salt.

The S segment complementary RNA exhibited a marginally reduced affinity with purified trimeric GST-N relative to S viral RNA at low salt, and the S complementary RNA-N interaction was significantly reduced at 180 mM NaCl. The M and L segment complementary RNAs exhibited significantly reduced affinity for trimeric GST-N compared with their viral RNA counterparts even at low NaCl concentrations. These data are consistent with the idea that recognition of the viral RNA by trimeric GST-N is required for selection of viral RNA and exclusion of complementary RNA during the encapsidation process. Viral RNA randomized, which mimics the overall secondary structure and stability of the S segment viral RNA, was not recognized with high affinity by trimeric GST-N. This observation, along with the observation that the complementary RNAs are not efficiently recognized by N, indicates that characteristics in addition to simple secondary structure are required for specific recognition of viral RNA by N.

Both secondary structure and primary sequence are required for panhandle-N interaction. The S, M, and L segment panhandles are double stranded but punctuated by single symmetrically opposed unpaired nucleotides at positions 9 and either 18 or 19 from the 5′ and 3′ termini. We constructed various mutations in the S segment viral RNA panhandle to examine the features of the viral RNA required for recognition by trimeric GST-N. RNA 14 contains three adjacent nucleotide substitutions near the 5′ end that would disrupt the terminal stem structure (Fig. 2A). We carried out simple RNA binding analysis with trimeric GST-N, similar to that shown in Fig. 1, to measure binding affinity for these RNAs. The data

FIG. 1. RNA binding profile of trimeric GST-N with the viral and complementary panhandles corresponding to the S, M, and L segments. (A) The nucleotide sequence and highly probable secondary structure of each of the RNAs is shown at the left. For each of the panhandle sequences, the nucleotides common to the both the complementary RNA (cRNA) and its antecedent viral RNA (vRNA) are shown in grey, while the nucleotides of the complementary RNA that vary relative to the viral RNA are shown in black. To generate viral RNA (randomized), the 5′ nucleotides of the S segment RNA were randomized and the 3′ nucleotides were chosen such that the secondary structure of the RNA would be the same as that of the viral RNA panhandle. Nucleotides that vary relative to those of the viral RNA panhandle are shown in black. (B) The RNA binding profiles as a function of increasing purified trimeric GST-N are shown in the right part of the figure. Increasing concentrations of purified trimeric GST-N were incubated with a constant concentration of ^{32}P-labeled RNA and protein-RNA complexes were isolated by filter binding as described in the Materials and Methods section. The data are plotted to show the binding profile at relatively high concentrations of trimeric GST-N and at 80 mM salt to display binding to complementary RNA and viral RNA (randomized). To determine the dissociation constants for the viral RNAs, the data were replotted to optimize visualization and analysis at lower trimeric GST-N concentrations. The data shown are from one experiment. However, each of the RNAs was analyzed in three separate experiments, and the measured K_ds with standard deviations are shown in Table 1.
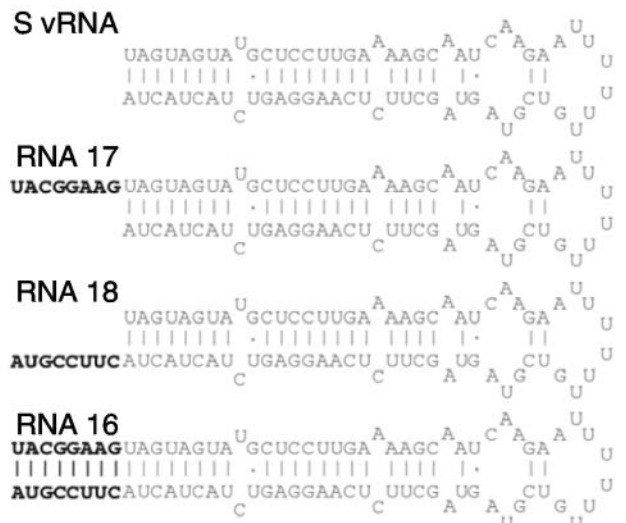
A
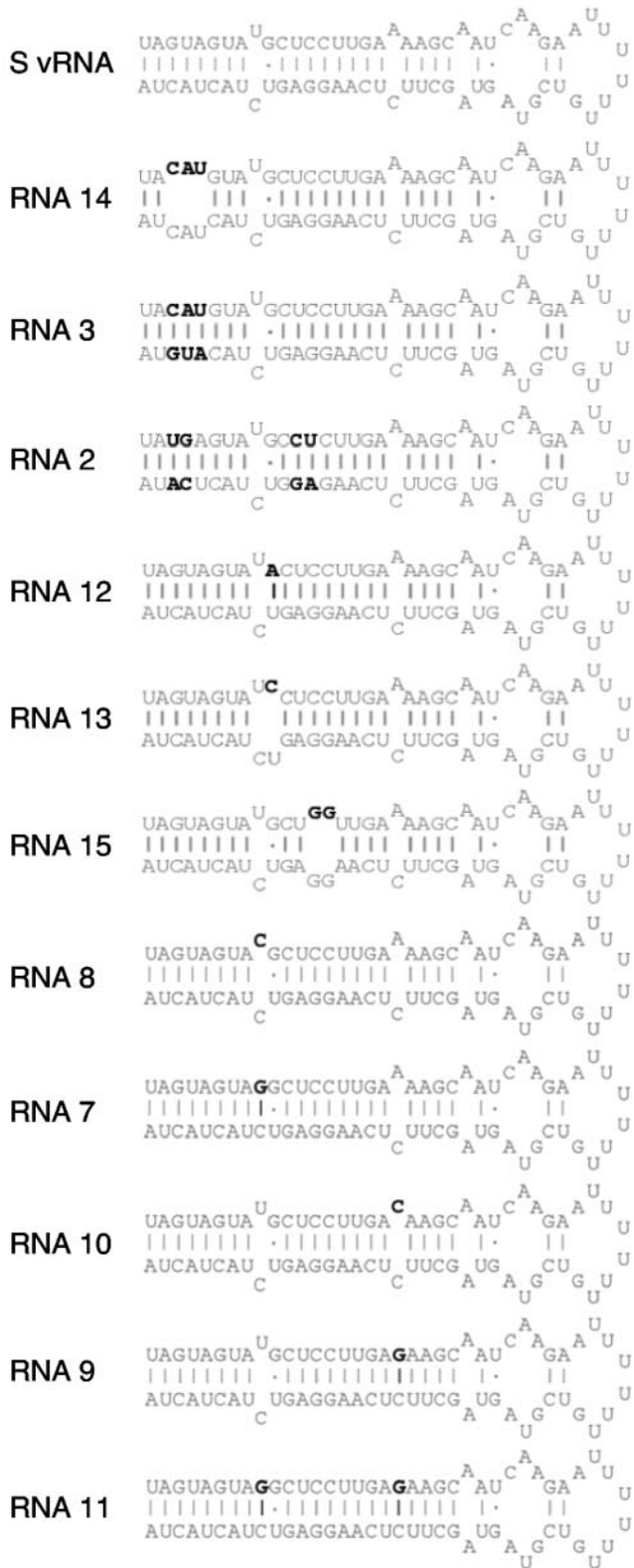
B
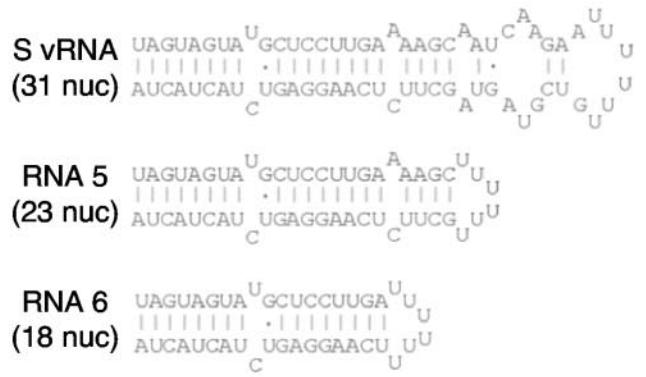
C

TABLE 1. Dissociation constants for purified trimeric Sin Nombre virus GST-N with minus-strand viral RNA (vRNA) or plus-strand complementary RNA (cRNA)

RNA	K_d (nM) at NaCl concn:		
	80 mM	160 mM	320 mM
S vRNA	39 ± 2	22 ± 1	38 ± 2
S cRNA	97 ± 1	250 ± 4	ND
S vRNA (randomized)	285 ± 5	ND	ND
M vRNA	18 ± 1	21 ± 1	27 ± 1
M cRNA	221 ± 4	483 ± 7	ND
L vRNA	30 ± 2	36 ± 2	27 ± 1
L cRNA	237 ± 5	712	ND
RNA 14	321 ± 6	ND	ND
RNA 3	319 ± 4	817 ± 8	ND
RNA 2	297 ± 5	719 ± 8	ND
RNA 12	27 ± 1	31 ± 1	39 ± 1
RNA 13	102 ± 2	271 ± 5	ND
RNA 15	371 ± 4	ND	ND
RNA 8	37 ± 1	27 ± 2	28 ± 2
RNA 7	60 ± 1	170 ± 3	339 ± 7
RNA 10	39 ± 1	29 ± 2	35 ± 1
RNA 9	57 ± 2	181 ± 6	415 ± 9
RNA 11	131	ND	ND
RNA 5	45 ± 1	39 ± 1	50 ± 1
RNA 6	719 ± 7	ND	ND
RNA 17	25 ± 1	33 ± 1	41 ± 2
RNA 18	29 ± 2	28 ± 1	39 ± 1
RNA 16	22 ± 1	31 ± 1	39 ± 2

[a] Values are from three independent experiments. ND, not done.
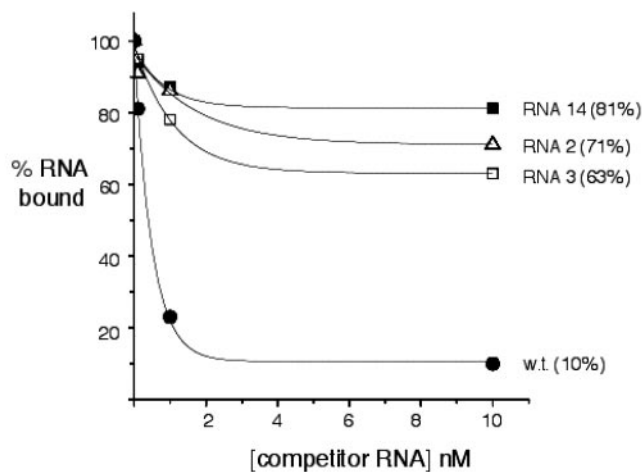

FIG. 3. RNA binding competition analysis of S segment viral RNA variants. As described in detail in the Materials and Methods section and the text, a constant amount of purified trimeric GST-N protein was incubated with a constant amount of labeled RNA corresponding to the wild-type viral RNA panhandle and increasing concentrations of unlabeled competitor RNA. The quantitative reduction of binding of trimeric GST-N to labeled RNA as a function of increasing competitor RNA was measured for each RNA. The figure depicts the competition curves for three of the variant RNAs and for the wild type. The competition curves for the other RNAs in Fig. 2 are not shown. However, the maximum extent of competition for all of the S segment panhandle variants is presented in Table 2. The data in the figure and in Table 2 are the averages of three separate experiments. The standard deviation for the measured values of all of the RNAs is presented in Table 2.

from this experiment indicated that RNA 14 was not recognized with high affinity (Table 1).

In addition, we performed competition binding experiments in which increasing amounts of unlabeled competitor RNA were added to binding reactions containing purified GST-N trimer and a constant amount of radiolabeled wild-type panhandle RNA; effective competition by the unlabeled RNA would result in reduction of binding of the labeled RNA to GST-N. This experiment indicated that mutant 14 did not effectively compete for binding to GST-N protein (Fig. 3). Thus, both the binding and competition data are consistent with a requirement for terminal base-pairing for specific recognition by N.

To see whether regeneration of a terminal stem was sufficient for recognition by N, we created a second-site mutant that retains the 5′ substitutions of RNA 14 and contains three additional changes in nucleotides 3, 4, and 5 from the 3′ end.

When present together in the panhandle, these nucleotide changes would restore terminal hydrogen bonding but create a stem of altered sequence (RNA 3) (Fig. 2A). In addition, we constructed a similar RNA in which alternative base pairs were created in the terminal stem as well as in the hydrogen-bonded nucleotides at positions 12 and 13 (RNA 2). RNA binding and competition analysis with these sequences indicated that these three RNAs were not recognized with high affinity by GST-N (Table 1 and Fig. 3). These data are consistent with a role for both primary sequence and secondary structure at the terminus of the panhandle in recognition by purified trimeric N.

In some hantavirus strains related to Sin Nombre virus, such as NY1, Puumala, Tula, and Andes (6, 11, 15, 21), an A residue rather than G is present at position 10 from the 5′ end of the RNA. This transition mutation would maintain the general panhandle configuration since there is a U residue at position 10 from the 3′ end of the RNA. RNA 12 contains such a G-to-A substitution at position 10 from the 5′ end (Fig. 2A). While viral RNA contains a single pair of unpaired nucleotides at position 9, in plus-strand Sin Nombre virus complementary

FIG. 2. Nucleotide variants in the S segment RNA panhandle. RNAs were synthesized as described in the Materials and Methods section. (A) Probable secondary structures of a set of RNAs containing nucleotide substitutions. Substitutions are shown in black. The RNAs shown in B are secondary structures of S segment viral RNA (vRNA) panhandles of decreasing length, as indicated. Panhandle RNAs containing additional nucleotides at the 5′ or 3′ terminus or both are shown in C. Additional nucleotides are indicated in black. The likely secondary structure of each of the RNAs was assessed by both P-num analysis and examination of alternative structures (Materials and Methods). The secondary structures of all of the RNAs except RNA 14 are highly probable. The three substitutions in RNA 14 would be expected to substantially disrupt base pairing such that the terminal two nucleotides would be unpaired in a substantial fraction of the RNA population.

TABLE 2. Competition analysis of Sin Nombre virus GST-N protein-RNA interactions[a]

Competitor RNA	Labeled RNA bound to N (% of wild-type value)
Wild-type S RNA	10 ± 1
RNA 14	81 ± 3
RNA 3	63 ± 2
RNA 2	71 ± 4
RNA 12	15 ± 2
RNA 13	59 ± 5
RNA 15	80 ± 6
RNA 8	18 ± 1
RNA 7	35 ± 2
RNA 10	19 ± 1
RNA 9	37 ± 3
RNA 11	59 ± 5
RNA 5	21 ± 1
RNA 6	73 ± 4
RNA 17	23 ± 2
RNA 18	19 ± 1
RNA 16	20 ± 3

[a] Increasing unlabeled RNAs were used in competition with ^{32}P-labeled wild-type RNA as in Fig. 3. The ability of each RNA to compete for binding to trimeric N is indicated by the maximal reduction in the binding of ^{32}P-labeled wild-type RNA. The results are based on three independent experiments.
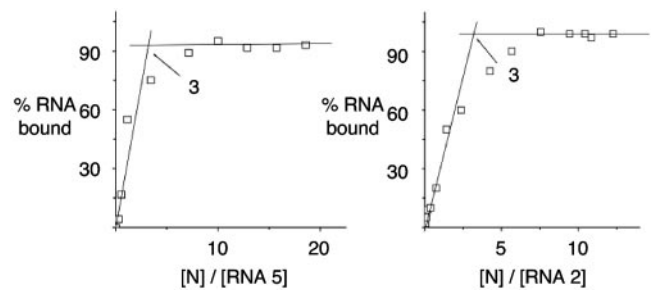

FIG. 4. Binding stoichiometry of trimeric N-panhandle interaction. The results from binding RNA experiments were replotted to determine stoichiometry as described in the Materials and Methods section. Data for RNA 5, which is bound by trimeric GST-N at high affinity, and RNA 2, which is bound at lower affinity, are shown. The data indicate that three monomers are bound per panhandle. Since the binding experiments were carried out with purified trimeric GST-N, this corresponds to 1 trimer/panhandle. The binding data for all of the RNAs analyzed were similarly plotted and indicated similar stoichiometry independent of binding affinity (not shown).

RNAs, nucleotides 9 and 10 are both unpaired. Thus, RNA 13 contains a G-to-C transversion such that in the viral RNA, nucleotide 10 along with nucleotide 9 would both remain unpaired. Finally, RNA 15 contains two consecutive C-to-G substitutions at positions 13 and 14 that would disrupt the nine-nucleotide-long, base-paired segment that begins at nucleotide 10. RNA 12 was recognized at high affinity by GST-N protein (Table 1) and competed with wild-type RNA for binding to GST-N protein (Table 2), indicating that an alternative base pair at position 10 does not affect the interaction with N. However, disruption of the stem structure (in mutants 13 and 15) resulted in a corresponding reduction in specific recognition by trimeric GST-N and the inability to compete efficiently with wild-type RNA for binding to trimeric GST-N (Tables 1 and 2).

To further examine the importance of the unpaired nucleotides at positions 9 and 19, which interrupt the double-stranded panhandle of S segment viral RNA, we constructed RNAs in which the nucleotides are altered but left unpaired or altered such that a longer uninterrupted double-stranded region was formed. In particular, nucleotide 9 from the 5′ end was changed from U to C (RNA 8) or to G (RNA 7). In RNA 7, base-pairing with the corresponding C on the 3′ side of the stem would occur. Similarly, nucleotide 19 from the 5′ end was changed from A to C (RNA 10) or to G (RNA 9) (Fig. 2A). Finally, the mutations present in both mutants 7 and 9 were simultaneously introduced such that an uninterrupted base-paired region 23 nucleotides in length was present (RNA 11).

The data from RNA binding experiments and binding competition experiments with these mutants are summarized in Tables 1 and 2. Interestingly, it appeared important for nucleotides 9 and 19 to remain unpaired for specific recognition by

trimeric GST-N. Substitution of a nucleotide that would retain nucleotides 9 and 19 in unpaired form (RNAs 8 and 10, respectively) resulted in RNAs that were recognized by trimeric N with high affinity even at increasing salt concentrations. In contrast, the introduction of base pairs at nucleotides 9 and 19 (RNAs 7, 9, and 11) resulted in RNAs that could not stably interact with trimeric GST-N at increasing salt concentrations. Taken together, these data suggest that overall secondary structure is important for recognition by trimeric N protein. However, nonconservative nucleotide substitutions in base-paired regions can markedly reduce the affinity of GST-N for the panhandle, indicative of a contribution of a primary sequence requirement for recognition by N.

Minimum panhandle size and stoichiometry of N-panhandle interaction. Based on previous work (23) and the data described here, a hantavirus panhandle composed of the terminal 32 nucleotides from both the 5′ and 3′ ends is sufficient as a substrate for trimeric N recognition. To determine the minimum size of panhandle required for recognition by trimeric N, we constructed RNAs that contained fewer interior nucleotides and carried out RNA binding studies with these RNAs. RNA 5 contains the terminal 23 nucleotides and RNA 6 contains the terminal 18 nucleotides of the panhandle, respectively (Fig. 2B). The results of this experiment indicated robust interaction between trimeric GST-N and RNA 5 but not RNA 6 (Tables 1 and 2). Thus, a panhandle 23 nucleotides in length is sufficient for recognition by trimeric N.

We attempted to determine the binding stoichiometry for N with its substrate panhandle with the shortest RNA that bound to trimeric GST-N with high affinity. We replotted the data from the RNA binding experiments with RNA 5 to calculate stoichiometry (Fig. 4). The plot is consistent with the binding of a trimer-to-panhandle ratio of 1:1. Similar data were obtained from stoichiometry plots with other panhandle RNAs that interact with trimeric GST-N protein at high specificity (data not shown). We also examined the binding stoichiometry of RNAs that were not recognized by trimeric N with high affinity. These also indicated a 1:1 stoichiometry. For example, see RNA 2 (Fig. 4)
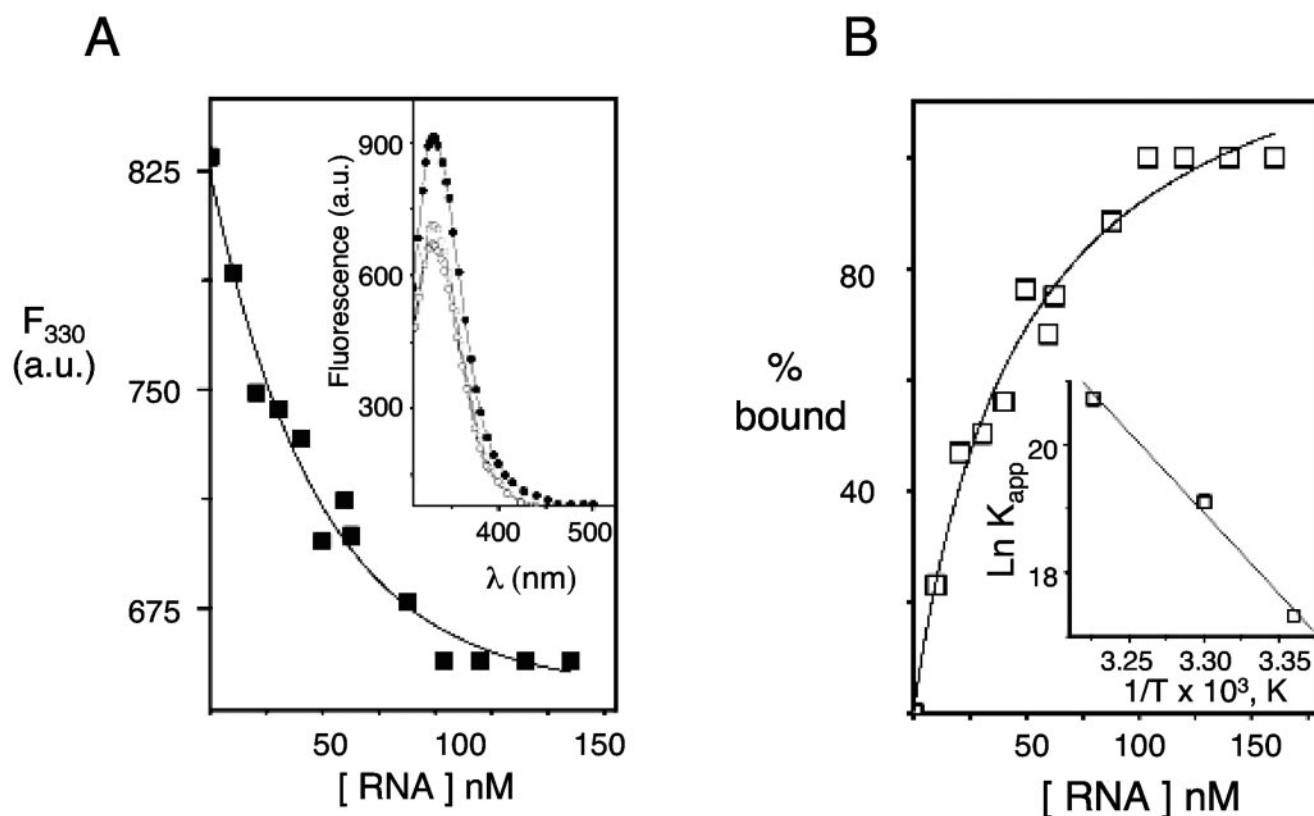
FIG. 5. Fluorescence spectroscopic and thermodynamic analysis of N protein trimer and S segment viral RNA panhandle association. **(A)** As described in the Materials and Methods section, a fixed concentration of N protein trimer in binding buffer was excited at 295 nm, and fluorescence intensity at 330 nm was recorded. The experiment was carried out at 25°C. The fluorescence signal from free binding buffer in the absence of GST-N protein trimer was subtracted where appropriate. The fluorescence intensity of the N protein trimer at 330 nm was monitored at different input concentrations of S segment Sin Nombre virus RNA panhandle. A plot of fluorescence intensity (at 330 nm) as a function of Sin Nombre virus S segment RNA panhandle concentration was then plotted in panel A. The inset shows the fluorescence emission spectra (λ_{ex} = 295 nm) of N protein trimer alone (■) and in the presence of S segment viral RNA panhandle at concentrations of 50 nM (○) and 110 nM (□). **(B)** The N protein bound at different input concentrations of S segment Sin Nombre virus RNA panhandle was calculated from panel A. A plot of the N protein bound at each input concentration of S segment Sin Nombre virus RNA panhandle is shown in panel B. The dissociation constant, corresponding to the concentration of S segment Sin Nombre virus RNA panhandle at which half of the N protein trimer is bound, was calculated from this binding profile (panel B). ln K_{app} ($1/K_d$) at three different temperatures was calculated. A plot of ln K_{app} versus $1/T$ (van't Hoff plot) is shown in the inset. ΔH and ΔS values were calculated from the van't Hoff plot as described in the Materials and Methods section. a.u., arbitrary units.

Addition of nucleotides to the 5′ and 3′ ends of the panhandle does not abolish recognition by N. Given that the panhandle is composed of the terminal nucleotides of the viral RNA, it seemed likely that recognition of the panhandle by trimeric N would be correspondingly dependent on terminal placement. To test this hypothesis, we added several nucleotides to either the 5′ end (RNA 17), the 3′ end (RNA 18), or both the 5′ and 3′ ends (RNA 16) (Fig. 2C). In the RNA containing additional nucleotides at both the 5′ and 3′ ends (RNA 16), the nucleotides that were added are capable of hydrogen bonding, thereby extending the length of the panhandle by 8 bp. Surprisingly, the addition of nucleotides to either terminus had no obvious effect on the affinity of binding by trimeric GST-N (Tables 1 and 2). Thus, recognition by N is not affected by displacement of the terminal nucleotides toward the interior of the RNA.

Binding of trimeric N to the panhandle is an entropy-driven process. We further investigated the interaction between trimeric N protein and S segment panhandle RNA with fluorescence spectroscopy. Essentially, we tried to examine the general conformation of trimeric GST-N in the absence and presence of panhandle RNA, as evidenced by the disposition of tryptophan as measured by excitation and emission spectra. N protein contains 10 tryptophan residues/polypeptide. Figure 5A (inset) shows the emission spectra of trimeric GST-N protein in the absence of RNA following excitation with light at a wavelength (λ) of 295 nm. Whereas free L-tryptophan exhibits an emission maximum of 350 nm (data not shown), GST-N protein yielded a λ_{max} of 330 nm. This N-dependent shift in λ_{max} is approximately twice that observed for most monomeric proteins (3, 41) and is consistent with the shielding of N-associated tryptophan in a trimeric protein.

We next examined the thermodynamic parameters associated with interaction between trimeric GST-N protein and the viral RNA panhandle. The addition of saturating concentrations of wild-type RNA to the GST-N protein trimer decreased the fluorescence quantum yield by 21% without a change in λ_{max} (Fig. 5A, inset). A similar effect but varying in magnitude
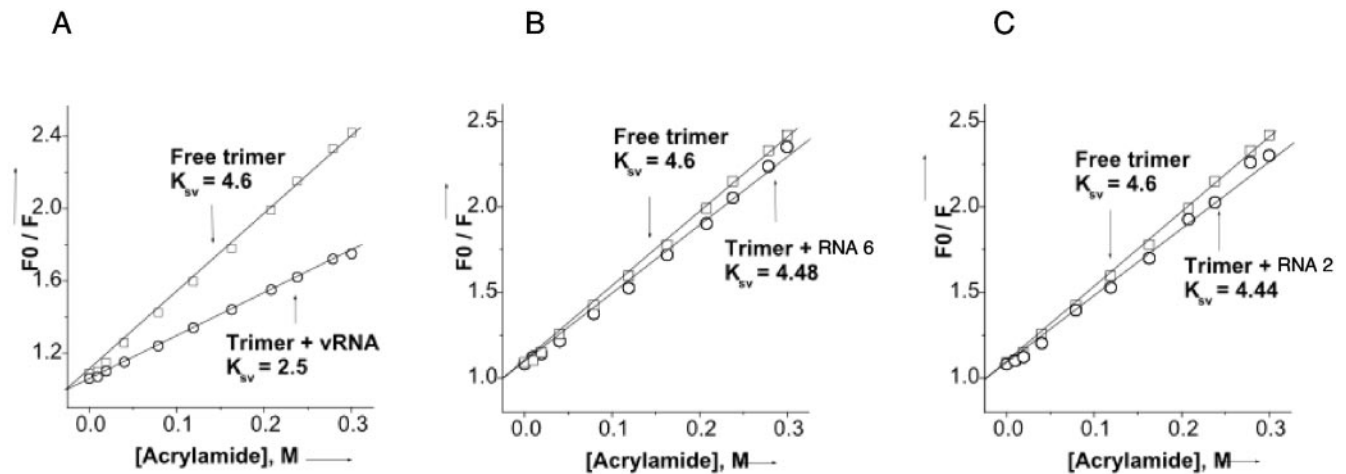
FIG. 6. Stern-Volmer plots of tryptophan fluorescence quenching of N protein trimer by acrylamide. A fixed concentration of trimeric GST-N in binding buffer was excited at 295 nm, and emission was recorded at 330 nm. The fluorescence studies were carried out at room temperature. The fluorescence signal from free binding buffer in absence of GST-N protein trimer was subtracted whenever required. The fluorescence intensity at 330 nm was determined at different input concentrations of acrylamide. Plots of F_0/F as a function of acrylamide concentration (Stern-Volmer plot) for free GST-N protein trimer in absence (□) and presence (○) of RNA of S segment Sin Nombre virus RNA panhandle (panel A), RNA 6 (panel B), and RNA2 (panel C) was used to calculate the Ksv values as described in the Materials and Methods section. The data shown are for viral RNA, RNA 6, and RNA 2 in graphs A, B, and C, respectively.

was observed with each of the panhandle RNAs listed in Table 1 (data not shown). The decrease in the fluorescence quantum yield at 330 nm with addition of different concentrations of wild-type minipanhandle RNA at 25°C is shown in Fig. 5A. The dissociation constants corresponding to the concentration of N protein at half saturation were calculated at three different temperatures. These data were then used to generate a van't Hoff plot (Fig. 5B) that was used to calculate the pertinent thermodynamic parameters ΔG, ΔH, and ΔS as described in the Materials and Methods section. This analysis indicated that $\Delta G = -10.4$ kcal/mol, $\Delta H = 49.9$ kcal/mol, and $\Delta S = 202.4$ entropy units. From these data it is evident that binding between the N protein trimer and the wild-type minipanhandle RNA is an entropy-driven process. The positive entropy change compensates for an observed positive enthalpy value and drives the binding reaction by a total free energy change of -10.5 kcal/mol at 25°C. These are characteristics consistent with the correct interaction of a substrate RNA with an RNA binding pocket of N.

To further compare the interaction of the panhandle RNAs with trimeric GST-N protein, we compared fluorescence quenching of N-associated tryptophan residues in the presence and absence of panhandle RNAs. Figure 6 depicts the effect of wild-type panhandle RNA on the fluorescence quenching of purified trimeric GST-N with increasing concentrations of acrylamide, an uncharged molecule that tends to quench accessible tryptophan residues. This analysis yielded a Stern-Volmer quenching constant (Ksv) of 4.6. The presence of panhandle RNA decreased the quenching of tryptophan by acrylamide, resulting in a Ksv of 2.5. This is consistent with a panhandle-dependent conformational change in trimeric N protein such that tryptophan residues are sequestered away from the surface of the protein following binding to the panhandle.

We determined the effect on Ksv for the panel of panhandle

variants that were previously characterized by RNA filter binding (Table 3). Significantly, there was generally good correspondence between those RNAs that were recognized by trimeric GST-N at high affinity, as evidenced by a low K_d, and those RNAs that exhibited a decreased Ksv relative to free protein. In particular, RNAs 5, 10, 12, and 16 all interacted with trimeric GST-N protein at high affinity and appeared to induce a conformational change in trimeric N similar to that

TABLE 3. Stern-Volmer quenching constants for the association of N protein trimers with different panhandle RNA molecules

RNA	Ksv (M^{-1})
Free trimer	4.60 ± 0.05
S viral RNA	2.10 ± 0.02
S complementary RNA	6.00 ± 0.11
S viral RNA (randomized)	7.00 ± 0.17
RNA 14	4.46 ± 0.05
RNA 3	4.50 ± 0.07
RNA 2	4.44 ± 0.09
RNA 12	3.00 ± 0.10
RNA 13	6.00 ± 0.20
RNA 15	4.50 ± 0.15
RNA 8	3.00 ± 0.10
RNA 7	4.19 ± 0.12
RNA 10	3.00 ± 0.05
RNA 9	5.40 ± 0.13
RNA 11	4.50 ± 0.11
RNA 5	3.00 ± 0.05
RNA 6	4.48 ± 0.13
RNA 17	4.20 ± 0.05
RNA 18	4.20 ± 0.10
RNA 16	2.70 ± 0.06

observed with the wild-type panhandle. This is indicative of similar correct, high-affinity recognition of these RNAs by trimeric N. However, the results with the set of mutants containing additional nucleotides at the 5′ end, the 3′ end, or both (RNAs 17, 18, and 16, respectively) were strikingly different. Each of these panhandle variants was recognized by trimeric GST-N with high affinity. However, only RNA 16, which contains extra nucleotides at both the 5′ and 3′ ends and would have an extended base-paired region, resulted in an apparent conformational change in N upon binding. In contrast, RNAs 17 and 18 were bound at high affinity by trimeric GST-N, but there was not a corresponding conformational alteration of N. These data are consistent with initial high-affinity binding of the panhandle by trimeric N followed by a conformational change in N. Mutants 17 and 18 are apparently proficient in the initial interaction with N but do not induce the subsequent conformational change in N.

DISCUSSION

Viral replication requires specific and efficient genome encapsidation. Trimeric hantavirus GST-N protein binds to the panhandles formed by the termini of each of the three genome segments with similar high affinity. Thus, during hantavirus RNA encapsidation, high-affinity recognition of the viral RNA panhandle by trimeric N likely mediates specific preferential encapsidation of the three viral minus strands and the segregation of plus-strand viral RNA and cellular RNA. Since all members of the *Bunyaviridae* can potentially form terminal panhandle structures, it is likely that similar recognition of the viral RNA panhandle by trimeric N is a key component in the specificity of RNA packaging for this virus family.

Plus-stranded complementary RNA can form panhandle structures similar in overall conformation and stability to those formed by the viral RNA but are recognized at lower affinity by trimeric N. What characteristics of the viral RNA panhandle account for specific recognition? Mutational analysis of the panhandle indicates that secondary structure and primary sequence are both important for recognition by trimeric GST-N. The terminal 23 nucleotides of the panhandle are sufficient for interaction with N, and for the S and M genome segments, all but two of these nucleotide positions contain hydrogen-bonded nucleotides. As might be expected, this extensive base-pairing is important for interaction with N, as evidenced by the introduction of nucleotides that abolish base pairing. However, it is also important that the four unpaired nucleotides of the panhandle, at positions 9 and 19, remain unpaired, since nucleotide substitutions that enable pairing at these positions result in concomitant inhibition of binding by trimeric N. In contrast, substitutions that maintain these nucleotides in an unpaired state allow high-affinity interaction with trimeric N.

The primary sequence of the base paired nucleotides is also important for specific recognition by trimeric N, since substitution with alternative paired nucleotides results in a substantial reduction in binding affinity by trimeric N. This role of primary sequence likely accounts for the differential binding affinity of trimeric N for the minus and plus strands. It is formally possible that an alternative tertiary RNA structure was formed following the introduction of alternative base pairs in the panhandle. However, substantial differences in tertiary

structure seem unlikely since the panhandle is marked by such extensive base-pairing. Double-stranded RNA typically assumes an A-form helix with a 28-Å pitch (42). With the exception of the nucleotide pairs at positions 9 and 19, the panhandle is double stranded, corresponding to an RNA that is approximately 650 Å in length. The introduction of alternative nucleotide pairs would be unlikely to alter this basic configuration. It is more likely that position-specific interaction between particular nucleotides and the amino acids in the RNA binding pocket of N is required for high-affinity interaction.

In addition to a probable role in encapsidation, recognition of the panhandle by N may function in RNA replication. Trimeric N might facilitate the formation of an initiation complex with the RNA-dependent RNA polymerase, the RNA panhandle, and a priming oligoribonucleotide derived by cap snatching. This would then enable the polymerase to initiate replication at the 3′ end of the RNA template within the panhandle. Such a role for N can be readily envisioned for the initiation of plus-strand synthesis since trimeric N recognizes the minus-strand panhandle with high affinity and also in minus-strand initiation, although the interaction between N and the plus-strand panhandle is of lower affinity.

Previously published work indicated that N protein from viruses of the *Hantavirus* and *Bunyavirus* genera preferentially binds to a signal(s) near the 5′ end of the S segment (26, 40). While the subunit composition of the bacterially expressed hexahistidine-tagged N used in these studies was not examined, it is likely that these protein preparations were composed of a mixture of monomeric, dimeric, and trimeric N. Comparison of the RNA binding affinity of unfractionated GST-N with the purified trimeric GST-N indicates that the trimer binds to the panhandle, while the mixed population binds to RNAs containing the viral RNA 5′ end (23). It is possible that monomeric and dimeric N functions in a way that is distinct from that of trimeric N during virus replication. However, since trimeric N appears to be a fundamental subunit intermediate leading to capsid formation (1, 19), we favor the idea that recognition of the viral RNA panhandle by the trimer is likely to provide the basis for specific RNA encapsidation.

The presence of a GST fused to N, which was used in our N expression construct, or a hexahistidine tag, which was used in previous studies to examine the interaction between N and RNA (12, 26, 35, 39, 40), could potentially affect the properties of N. In the present instance, it is most pertinent to consider the possibility that the presence of the GST tag affected either the trimerization of N or the ability of purified trimeric N to recognize the viral panhandle RNA with specificity. We recently initiated experiments with N protein expressed from the bone fide start and stop codons of the Sin Nombre virus N gene. Thus, the resulting protein is devoid of additional amino acids. Preliminary sucrose sedimentation of this protein indicates a peak fraction at approximately 150 kDa, consistent with the formation of trimers, and preliminary RNA binding properties of the purified trimer with S and M segment viral RNA and complementary RNA yield K_d values virtually identical to those measured for purified trimeric GST-N (data not shown).

The panhandle RNAs that we analyzed were generated by T7 RNA polymerase. As with other RNA polymerases, initiation can typically occur at several nucleotides near the formal +1 position of the T7 promoter (13, 30). Thus, the RNAs that

we examined are very likely to be composed of a population of RNAs with 5′ termini that differ by one or several nucleotides. Given this likely heterogeneity, it is possible that only some of the molecules in the RNA population which initiate at a particular 5′ nucleotide are preferentially bound by trimeric GST-N. However, the addition of nucleotides to the 5′ end (RNA 17) did not affect recognition by trimeric N. In addition, the 5′ end of viral RNA synthesized during virus infection contains heterogenous 5′ ends that arise from initiation of cellular RNAs by a putative cap-snatching mechanism (7, 8, 16). Thus, it is likely that the termini of the panhandle need not be formed with precision for specific recognition by trimeric N. Nonetheless, without direct sequencing of all the RNAs, it is possible that the substitution of specific nucleotides close to the +1 position might have led to an unexpectedly large effect on the distribution of initiation sites for a specific RNA.

If one assumes that trimeric N protein is globular, the approximate theoretical diameter of trimeric N protein is 80 to 100 Å. Potentially, there would be space for several trimers along the length of the predominantly double-stranded RNA panhandle. However, the binding stoichiometry appears to be consistent instead with the binding of a single trimer per panhandle. Capsid formation would involve both trimer RNA interaction and interaction between multiple N molecules. It seems likely that the specific in vitro interaction between trimeric N and the RNA panhandle represents an initial step in RNA encapsidation. In vivo, such a complex between N and the panhandle may serve as a nucleation point for subsequent intermolecular interaction between multiple N molecules, resulting in capsid assembly.

Though the panhandle by definition is composed of the terminal nucleotides of the viral RNA, the structure need not be located at the RNA terminus for high-affinity recognition by trimeric N, since the addition of nucleotides to either the 5′ end, the 3′ end, or both did not measurably inhibit binding by N. However, the fact that trimeric N recognizes the terminal sequences with specificity likely reflects a role for N protein at that site in the RNA distinct from encapsidation. In particular, binding to the panhandle is consistent with a role for trimeric N protein in either initiation of plus-strand RNA at the 3′ end of the viral RNA template, termination at the 5′ end, or in both events.

Based on the thermodynamic events that occur during binding of the panhandle to the trimer, the protein-RNA interaction is an entropy-driven process. The most conventional interpretation of the data is that, in the absence of RNA, the amino acids constituting the RNA binding pocket of N are occupied by water molecules. Interaction of RNA with the binding pocket would then result in displacement of the water molecules, resulting in the measured increase in entropy. Based on the fluorescence quenching data, RNA-protein interaction also results in an apparent conformational change in N, as evidenced by the general redistribution of the tryptophan molecules to positions inaccessible to an uncharged quencher. Interestingly, the addition of nucleotides to either the 5′ or 3′ end of the panhandle did not diminish high-affinity binding by trimeric GST-N. However, the presence of these extra nucleotides abolished the conformational change in GST-N. Thus, it appears that the interaction between N and the panhandle results in initial high-affinity binding followed by protein rearrangement.

The simultaneous addition of complementary nucleotides to both the 5′ and 3′ ends of the panhandle such that a longer double-stranded RNA was created had no apparent effect on either binding affinity or subsequent conformational change in N. This differential effect of the addition of double-stranded versus single-stranded RNA on the conformational alteration of N is intriguing and suggests that rearrangement of N is dependent on interaction between double-stranded regions of the panhandle and the RNA binding site of N. It is likely that concurrent addition of no complementary nucleotides to the 5′ and 3′ ends would also abolish the rearrangement of N.

The formation of the panhandle and its recognition by trimeric N provide a simple and attractive model to account for specificity during viral RNA encapsidation. However, it is not clear how the panhandle forms. Thermodynamic calculations indicate that the highest negative free energy states for all three viral RNAs involve the formation of a panhandle. However, random intramolecular interaction is unlikely to drive panhandle formation, especially for an RNA as long as the hantavirus L segment. The efficient formation of a panhandle likely involves the activity of an RNA chaperone, a molecule that facilitates the rearrangement of RNA to allow the refolding of RNA to its most stable forms. Such a chaperone activity has been implicated in the correct folding of other viral RNAs and is associated with the viral nucleocapsid protein (5, 34). For hantaviruses and other members of the *Bunyaviridae*, such a chaperone activity most likely similarly resides in the N protein itself.

REFERENCES

1. **Alfadhli, A., Z. Love, B. Arvidson, J. Seeds, J. Willey, and E. Barklis.** 2001. Hantavirus nucleocapsid protein oligomerization. J. Virol. **75:**2019–2023.
2. **Botten, J., K. Mirowsky, D. Kusewitt, M. Bharadwaj, J. Yee, R. Ricci, R. M. Feddersen, and B. Hjelle.** 2000. Experimental infection model for Sin Nombre hantavirus in the deer mouse (Peromyscus maniculatus). Proc. Natl. Acad. Sci. USA **97:**10578–10583.
3. **Bougie, I., and M. Bisaillon.** 2003. Initial binding of the broad spectrum antiviral nucleoside ribavirin to the hepatitis C virus RNA polymerase. J. Biol. Chem. **278:**52471–52478.
4. **Chizhikov, V. E., C. F. Spiropoulou, S. P. Morzunov, M. C. Monroe, C. J. Peters, and S. T. Nichol.** 1995. Complete genetic characterization and analysis of isolation of Sin Nombre virus. J. Virol. **69:**8132–8136.
5. **Cristofari, G., R. Ivanyi-Nagy, C. Gabus, S. Boulant, J. P. Lavergne, F. Penin, and J. L. Darlix.** 2004. The hepatitis C virus Core protein is a potent nucleic acid chaperone that directs dimerization of the viral (+) strand RNA in vitro. Nucleic Acids Res. **32:**2623–2631.
6. **Dekonenko, A., V. Yakimenko, A. Ivanov, V. Morozov, P. Nikitin, S. Khasanova, T. Dzagurova, E. Tkachenko, and C. Schmaljohn.** 2003. Genetic similarity of Puumala viruses found in Finland and western Siberia and of the mitochondrial DNA of their rodent hosts suggests a common evolutionary origin. Infect. Genet. Evol. **3:**245–257.
7. **Dunn, E. F., D. C. Pritlove, H. Jin, and R. M. Elliott.** 1995. Transcription of a recombinant bunyavirus RNA template by transiently expressed bunyavirus proteins. Virology **211:**133–143.
8. **Garcin, D., M. Lezzi, M. Dobbs, R. M. Elliott, C. Schmaljohn, C. Y. Kang, and D. Kolakofsky.** 1995. The 5′ ends of Hantaan virus (*Bunyaviridae*) RNAs suggest a prime-and-realign mechanism for the initiation of RNA synthesis. J. Virol. **69:**5754–5762.
9. **Gavrilovskaya, I. N., M. Shepley, R. Shaw, M. H. Ginsberg, and E. R. Mackow.** 1998. β3 integrins mediate the cellular entry of hantaviruses that cause respiratory failure. Proc. Natl. Acad. Sci. USA **95:**7074–7079.
10. **Goldsmith, C. S., L. H. Elliott, C. J. Peters, and S. R. Zaki.** 1995. Ultrastructural characteristics of Sin Nombre virus, causative agent of hantavirus pulmonary syndrome. Arch. Virol. **140:**2107–2122.

11. **Gonzalez Della Valle, M., A. Edelstein, S. Miguel, V. Martinez, J. Cortez, M. L. Cacace, G. Jurgelenas, S. S. Estani, and P. Padula.** 2002. Andes virus associated with hantavirus pulmonary syndrome in northern Argentina and determination of the precise site of infection. Am. J. Trop. Med. Hyg. **66:**713–720.

12. **Gott, P., R. Stohwasser, P. Schnitzler, G. Darai, and E. K. Bautz.** 1993. RNA binding of recombinant nucleocapsid proteins of hantaviruses. Virology **194:**332–337.

13. **Helm, M., H. Brule, R. Giege, and C. Florentz.** 1999. More mistakes by T7 RNA polymerase at the 5′ ends of in vitro-transcribed RNAs. RNA **5:**618–621.

14. **Hewlett, M. J., R. F. Pettersson, and D. Baltimore.** 1977. Circular forms of Uukuniemi virion RNA: an electron microscopic study. J. Virol. **21:**1085–1093.

15. **Huang, C., W. P. Campbell, R. Means, and D. M. Ackman.** 1996. Hantavirus S RNA sequence from a fatal case of HPS in New York. J. Med. Virol. **50:**5–8.

16. **Hutchinson, K. L., C. J. Peters, and S. T. Nichol.** 1996. Sin Nombre virus mRNA synthesis. Virology **224:**139–149.

17. **Jaeger, J. A., D. H. Turner, and M. Zuker.** 1990. Predicting optimal and suboptimal secondary structure for RNA. Methods Enzymol. **183:**281–306.

18. **Jin, H., and R. M. Elliott.** 1993. Characterization of Bunyamwera virus S RNA that is transcribed and replicated by the L protein expressed from recombinant vaccinia virus. J. Virol. **67:**1396–1404.

19. **Kaukinen, P., V. Koistinen, O. Vapalahti, A. Vaheri, and A. Plyusnin.** 2001. Interaction between molecules of hantavirus nucleocapsid protein. J. Gen. Virol. **82:**1845–1853.

20. **Kaukinen, P., A. Vaheri, and A. Plyusnin.** 2003. Mapping of the regions involved in homotypic interactions of Tula hantavirus N protein. J. Virol. **77:**10910–10916.

21. **Kukkonen, S. K., A. Vaheri, and A. Plyusnin.** 1998. Completion of the Tula hantavirus genome sequence: properties of the L segment and heterogeneity found in the 3′ termini of S and L genome RNAs. J. Gen. Virol. **79:**2615–2622.

22. **Lakowicz, J. R.** 1999. Principles of fluorescence spectroscopy, p. 237–265. Plenum Press, New York, N.Y.

23. **Mir, M. A., and A. T. Panganiban.** 2004. Trimeric hantavirus nucleocapsid protein binds specifically with the viral RNA panhandle. J. Virol. **78:**8281–8288

24. **Mir, M. A., and D. Dasgupta.** 2001. Association of the anticancer antibiotic chromomycin A(3) with the nucleosome: role of core histone tail domains in the binding process. Biochemistry **40:**11578–11585.

25. **Obijeski, J. F., D. H. Bishop, F. A. Murphy, and E. L. Palmer.** 1976. Structural proteins of La Crosse virus. J. Virol. **19:**985–997.

26. **Osborne, J. C., and R. M. Elliott.** 2000. RNA binding properties of bunyamwera virus nucleocapsid protein and selective binding to an element in the 5′ terminus of the negative-sense S segment. J. Virol. **74:**9946–9952.

27. **Palmenberg, A. C., and J. Y. Sgro.** 1997. Topological organization of picor-naviral genomes: statistical prediction of RNA structural signals. Semin. Virol. **8:**231–241.

28. **Persson, R., and R. F. Pettersson.** 1991. Formation and intracellular transport of a heterodimeric viral spike protein complex. J. Cell Biol. **112:**257–266.

29. **Pettersson, R. F., and C. H. von Bonsdorff.** 1975. Ribonucleoproteins of Uukuniemi virus are circular. J. Virol. **15:**386–392.

30. **Pleiss, J. A., M. L. Derrick, and O. C. Uhlenbeck.** 1998. T7 RNA polymerase produces 5′ end heterogeneity during in vitro transcription from certain templates. RNA **4:**1313–1317.

31. **Raju, R., and D. Kolakofsky.** 1989. The ends of La Crosse virus genome and antigenome RNAs within nucleocapsids are base paired. J. Virol. **63:**122–128.

32. **Ravkov, E. V., S. T. Nichol, and R. W. Compans.** 1997. Polarized entry and release in epithelial cells of Black Creek Canal virus, a New World hantavirus. J. Virol. **71:**1147–1154.

33. **Ravkov, E. V., S. T. Nichol, C. J. Peters, and R. W. Compans.** 1998. Role of actin microfilaments in Black Creek Canal virus morphogenesis. J. Virol. **72:**2865–2870.

34. **Rein, A., L. E. Henderson, and J. G. Levin.** 1998. Nucleic-acid-chaperone activity of retroviral nucleocapsid proteins: significance for viral replication. Trends Biochem. Sci. **23:**297–301.

35. **Richmond, K. E., K. Chenault, J. L. Sherwood, and T. L. German.** 1998. Characterization of the nucleic acid binding properties of tomato spotted wilt virus nucleocapsid protein. Virology **248:**6–11.

36. **Schmaljohn, C., and B. Hjelle.** 1997. Hantaviruses: a global disease problem. Emerg. Infect. Dis. **3:**95–104.

37. **Schmaljohn, C. M.** 1996. Molecular biology of hantaviruses. Plenum Press, New York, N.Y.

38. **Schmaljohn, C. S., A. L. Schmaljohn, and J. M. Dalrymple.** 1987. Hantaan virus M RNA: coding strategy, nucleotide sequence, and gene order. Virology **157:**31–39.

39. **Severson, W., L. Partin, C. S. Schmaljohn, and C. B. Jonsson.** 1999. Characterization of the Hantaan nucleocapsid protein-ribonucleic acid interaction. J. Biol. Chem. **274:**33732–33739.

40. **Severson, W. E., X. Xu, and C. B. Jonsson.** 2001. cis-Acting signals in encapsidation of Hantaan virus S-segment viral genomic RNA by its N protein. J. Virol. **75:**2646–2652.

41. **Weisshart, K., A. A. Kuo, G. R. Painter, L. L. Wright, P. A. Furman, and D. M. Coen.** 1993. Conformational changes induced in herpes simplex virus DNA polymerase upon DNA binding. Proc. Natl. Acad. Sci. USA **90:**1028–1032.

42. **Westhof, E., and P. Auffinger.** 2000. RNA tertiary structure, p. 5222–5232. *In* R. A. Meyers (ed.), Encyclopedia of analytical chemistry. John Wiley & Sons, Chichester, England.

43. **Xu, X., W. Severson, N. Villegas, C. S. Schmaljohn, and C. B. Jonsson.** 2002. The RNA binding domain of the hantaan virus N protein maps to a central, conserved region. J. Virol. **76:**3301–3308.